

A Novel 9-MC-3 and 15-MC-6 Onset Stacked Metallacrown Single-Molecule Magnet: Synthesis and Crystal Structure

Suna Wang,^{†,‡} Lingqian Kong,[§] Hua Yang,[†] Zhoutong He,[⊥] Zheng Jiang,[⊥] Dacheng Li,^{*,†} Suyuan Zeng,[†] Meiju Niu,[†] You Song,^{*,‡} and Jianmin Dou^{*,†}

[†]School of Chemistry and Chemical Engineering, Liaocheng University, 252059 Liaocheng, People's Republic of China

[‡]State Key Laboratory of Coordination Chemistry, School of Chemistry and Chemical Engineering, Nanjing National Laboratory of Microstructures, Nanjing University, 210093 Nanjing, People's Republic of China

[§]Department of Chemistry and Biology, Dongchang College of Liaocheng University, 252059 Liaocheng, People's Republic of China

[⊥]Shanghai Synchrotron Radiation Facility, 201204 Shanghai, People's Republic of China

S Supporting Information

ABSTRACT: A novel enneanuclear manganese complex, $[\text{Mn}_9\text{O}_4(\text{Mesao})_6(\text{MeO})_3(\text{O}_2\text{CMe})_3(\text{OH})(\text{MeOH})_2] \cdot 2.5\text{-DMF}$ [**1**; Me-saoH₂ = 2-hydroxyphenylethanone oxime], was synthesized. The structure of **1** contains an unusual $[\text{Mn}_9\text{O}_4]$ core with an unprecedented defective “supertetrahedron” topology based on two parallel, onset stacked 9-MC-3 and 15-MC-6 metallacrown subunits. Magnetic studies indicate that **1** behaves as a single-molecule magnet.

Since Pecoraro and Lah first reported the examples of metallacrowns (MCs), $[\text{VO}(\text{shi})(\text{MeOH})_3]$ (9-MC-3) and $\text{Mn}(\text{OAc})_2[\text{Mn}_4(\text{shi})_4(\text{DMF})_6] \cdot 2\text{DMF}$ (12-MC-4) (shi = salicylhydroxamic acid and DMF = *N,N*-dimethylformamide), this family of metallamacrocycles has received considerable attention for their diverse architectures and potential applications.^{1–3} The traditional MCs have a $[\text{M}-\text{N}-\text{O}]_n$ repeated unit, and the cyclic structures range from 9-MC-3 to 24-MC-8. With the extension of crown ethers to azacrown and thiocrown ethers, the connectivity has grown to include a great variety of bridges, such as $-\text{[N-N]}-$, $-\text{[N-C-N]}-$, $-\text{[N-C-O]}-$, $-\text{[O-C}_m\text{-O]}-$, and $-\text{[X]}-$ (where X is a nonmetal atom). The structural types are also diversified, including 8-MC-4, 12-MC-3, 15-MC-6, 18-MC-9, 24-MC-12, 60-MC-20, and so on.^{2b} There are also examples of a few novel MCs in which simple MCs are fused together by M–O bonds to form dimers or sandwich complexes.^{2d–g}

Meanwhile, polynuclear clusters have attracted considerable attention in the recent decade because some of them can function as single-molecule magnets (SMMs), with magnetic hysteresis arising from the slow magnetization reversal spanning a high energy barrier, which is related to the easy-axis anisotropy *D* and large ground-state spin *S*.^{4,5} The typical nature of the MCs is that a molecule has a large number of metal ions within a small volume that can interact to provide a large spin. Inclusion of Mn^{III} ions with Jahn–Teller (JT) axes or lanthanide ions with strong spin–orbital coupling may also lead to high magneto-anisotropy. Up to now, a few 9-MC-3, 12-MC-4, 15-MC-5 and 14-MC-5 based on Mn^{III} and Ln^{III} ions behave as SMMs.^{2b,6–8} Herein we report a new manganese complex, $[\text{Mn}_9\text{O}_4(\text{Me-sao})_6$ -

$(\text{MeO})_3(\text{O}_2\text{CMe})_3(\text{OH})(\text{MeOH})_2] \cdot 2.5\text{DMF}$ (**1**), which contains 9-MC-3 and 15-MC-6 onset stacked MCs and shows SMM properties.

The reaction of $\text{Mn}(\text{OAc})_2 \cdot 4\text{H}_2\text{O}$ with Me-saoH₂ (2-hydroxyphenylethanone oxime) in MeOH/DMF at room temperature afforded black single crystals of **1** in 65% yield.⁹ The molecular structure of **1** (Figure 1) consists of nine Mn^{III} ions connected by six Me-Sao²⁻ ligands, one $\mu_3\text{-O}^{2-}$, three $\mu_4\text{-O}^{2-}$, three $\mu_2\text{-MeO}^-$, and three $\mu_2\text{-OAc}^-$ ions as well as one OH⁻ and two MeOH ligands. Three Mn1 ions are linked through one central $\mu_3\text{-O}^{2-}$ ion and three $\mu_4\text{-}\eta^2\text{:}\eta^1\text{:}\eta^2\text{-Me-Sao}^{2-}$ ligands, leading to a common triangular $[\text{Mn}^{\text{III}}_3(\mu_3\text{-O})(\mu_4\text{-ON})_3]^\ddagger$ core with a $(-\text{Mn}-\text{O}-\text{N})_3$ ring, a 9-MC-3 configuration. The Mn–N–O–Mn torsion angles are 43.7(4)°. Adjacent Mn2 and Mn3 ions are linked via $\mu\text{-}\eta^1\text{:}\eta^1\text{-Me-Sao}^{2-}$ and $\mu\text{-MeO}^-$ ions alternately, generating a novel 15-MC-6 ring with three $[\text{Mn}-\text{N}-\text{O}-\text{Mn}-\text{O}]$ repeated units. Six Mn ions are almost coplanar and arranged in a larger triangle with three Mn2 ions at the vertexes and three Mn3 ions at the edges, respectively. Within the triangle, every group of two Mn2 and one Mn3 neighboring ions are also bridged by one $\mu_4\text{-O}^{2-}$ ion. Consequently, a novel $[\text{Mn}^{\text{III}}_6(\mu_4\text{-O})_3(\mu_3\text{-ON})_3(\mu\text{-O})_3]^{3+}$ core is formed. Three carboxylates “cap” the large triangle core, bridging Mn2/Mn3A in a $\mu\text{-}\eta^1\text{:}\eta^1$ fashion. The Mn–N–O–Mn torsion angles are 25.2(5)°, much smaller than those of the $[\text{Mn}_3\text{O}]$ core. The Mn–O–Mn angles are in the range of 97.0(2)–132.9(3)°. This arrangement is largely different from those commonly reported $[\text{Mn}_6\text{O}_2]$ cores, which are usually formed by an offset arrangement of two $[\text{Mn}_3\text{O}]$ triangular cores.⁷

Two triangular cores are connected to each other through three “central” $\mu_4\text{-O}^{2-}$ ions and three “peripheral” phenolato O atoms as well as three “peripheral” oxime O atoms of Me-Sao²⁻ ligands to form an overall $[\text{Mn}^{\text{III}}_9(\mu_4\text{-O})_3(\mu_3\text{-O})(\mu\text{-O})_3(\mu_3\text{-ON})_6]^{4+}$ core with 9-MC-3 and 15-MC-6 in a parallel, onset stacking arrangement. All Mn ions are six-coordinated with a distorted octahedral geometry, and the JT axes are approximately parallel and perpendicular to both MC planes. The metal oxidation states were deduced from the meric parameters and charge-balance considerations, which were confirmed by bond

Received: August 10, 2010

Published: March 03, 2011

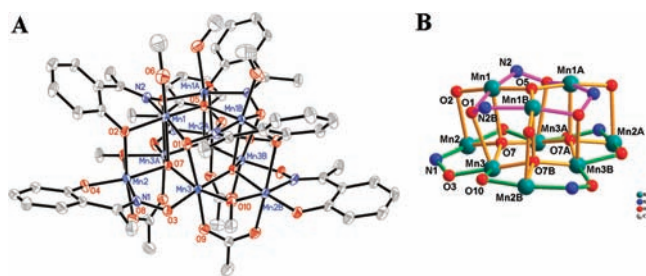


Figure 1. Left: ORTEP diagram of **1** with ellipsoids at the 30% probability level. Color code: gray, carbon; blue, nitrogen; red, oxygen; sky blue, manganese. Right: Core highlighting the MC ring. Symmetry codes: A, $1 - z, 1 - x, y$; B, $1 - y, z, 1 - x$.

valence sum (BVS) calculations and further X-ray absorption fine structure (XAFS) measurements (Table S1 and Figure S1 in the Supporting Information). Additional ligation about the core is provided by disordered terminal MeOH molecules and OH groups at Mn1 ions.

It should be noted that, to the best of our knowledge, **1** is the first structurally characterized fused MC with 9-MC-3 and 15-MC-6. Topologically, this arrangement can be regarded as part of a “supertetrahedron” missing a vertex from the tetrahedron. Thus, this complex joins only very limited manganese clusters with regular, distorted or defective “supertetrahedron” Mn_{10} and Mn_8 structures,¹⁰ and represents a new member of Mn_9 family.¹¹ Such a specific bridging mode may provide an opportunity to obtain interesting magnetic properties different from that of structures containing nonplanar $[Mn_6O_2]$ cores.

The temperature dependence of magnetic susceptibilities of **1** was measured on powdered polycrystalline samples in the temperature range of 2.5–300 K in a magnetic field of 1 kOe (Figure 2). The $\chi_M T$ value steadily decreases from 23.40 $\text{cm}^3 \text{K mol}^{-1}$ at 300 K both MC planes 18.27 $\text{cm}^3 \text{K mol}^{-1}$ at 40 K, indicating dominant antiferromagnetic exchange interactions. Upon cooling, $\chi_M T$ remains constant and then abruptly decreases to 16.52 $\text{cm}^3 \text{K mol}^{-1}$ at 2.5 K (Figure 2). The value at 40 K is suggestive of a ground state of $S \approx 6$, which may be rationalized by assuming both ferromagnetic and antiferromagnetic interactions between the nine Mn ions, and strongly dependent on the Mn–N–O–Mn torsion angles⁷ as well as Mn–O–Mn angles (Figure S3 in the Supporting Information).¹² Furthermore, the magnetic susceptibilities above 50 K can be fitted well by the Curie–Weiss law $\chi = C/(T - \theta)$, obtaining $C = 25.19 \text{ cm}^3 \text{K mol}^{-1}$ and $\theta = -24.80 \text{ K}$ (Figure S2 in the Supporting Information).

Because of the complexity of the system, an attempt to calculate the coupling constant between Mn^{III} ions was very difficult. We concentrated instead on characterizing the ground-state spin, S , and the zero-field-splitting (ZFS) parameter, D . The measurements of magnetization (M) versus the direct-current (dc) field were carried out for **1** in the ranges of magnetic field (H) from 1 to 7 T and at temperatures from 10 to 1.8 K, respectively. The reduced magnetization ($M/N\mu_B$) versus H/T demonstrates the nonsuperposition of the isofield lines and the presence of significant ZFS. The data were fitted by matrix diagonalization using the ANISOFT program, including isotropic Zeeman interactions, axial ZFS ($D\hat{S}_z^2$), and a full powder average of the magnetization, when assuming that only the ground state is populated at these temperatures and magnetic fields. The best fit was obtained with $S = 6$, $g = 1.99$, and $D = -0.78 \text{ cm}^{-1}$, indicating that the populations of low-lying excited

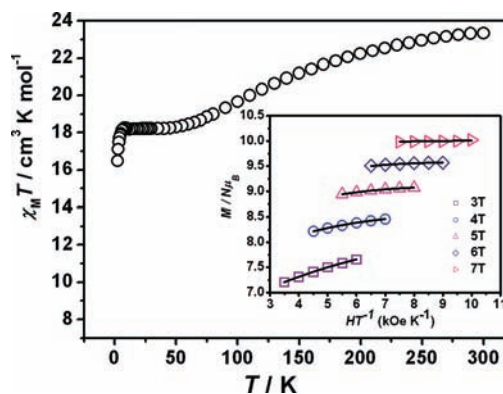


Figure 2. Plot of $\chi_M T$ vs T of **1** in an applied field of 2 kOe. Inset: Plot of the reduced magnetization ($M/N\mu_B$) vs H/T at the indicated applied fields. The solid lines represent the best-fit calculations.

states at 1.8–5.0 K are low and/or the intermolecular interactions are relatively small.

To probe the magnetization dynamics of **1**, alternating-current (ac) magnetic measurements were performed in a zero-applied dc field with a 5.0 Oe ac field oscillating at frequencies in the range of 1–1488 Hz and in the temperature range of 1.8–10.0 K. The in-phase (χ_M') and out-of-phase (χ_M'') signals versus T curves reveal that below $\sim 4.0 \text{ K}$ both χ_M' and χ_M'' are strongly frequency-dependent (Figure S4 in the Supporting Information). As the frequency (f) of the ac field was changed from 1488 to 1 Hz, the χ_M'' peak temperature (T_p) shifted from 2.99 to 1.84 K. A quantity given by $(\Delta T_p/T_p)/\Delta(\log f)$ is estimated to be 0.18, which falls in the range of a superparamagnet, and excludes the possibility of a spin glass.¹³ The (χ_M') signal decreases upon a decrease in the temperature, indicating the presence of low-lying excited states with larger S values than that in the ground state. Extrapolating the in-phase curve to 0 K from 7 K gives a $\chi_M' T$ value of 18.50 $\text{cm}^3 \text{K mol}^{-1}$, obtaining a ground state of $S \approx 6$, in good agreement with the dc result. The Arrhenius equation of $\tau = \tau_0 \exp(\Delta E_{\text{eff}}/k_B T)$ (where $\tau = 1/2\pi f$, ΔE_{eff} is the effective energy barrier for the magnetization relaxation, and τ_0 is the preexponential factor) was employed to extract relevant parameters with a slow magnetic relaxation. The results show that there is a linear correlation of $1/T_p$ versus $\ln(2\pi f)$ and the parameters are $\Delta E_{\text{eff}} = 35.20 \text{ K}$ and $\tau_0 = 8.5 \times 10^{-10} \text{ s}$ (Figure S5 in the Supporting Information). Moreover, the Cole–Cole plot of (χ_M') versus (χ_M'') signal exhibits a semicircular shape (inset of Figure 3), which was well fitted by a Debye model to give α parameters of 0.30–0.41. It is noticeable that ΔE_{eff} and D for **1** are larger than those of previously reported Mn_9 clusters (which are in the range 25–27 K and 0.23–0.29 cm^{-1} , respectively).^{11a–c}

In conclusion, we have reported an unusual $[Mn_9O_4]$ cluster with an unprecedented defective “supertetrahedron” topology based on two parallel, onset stacked 9-MC-3 and 15-MC-6 subunits. The magnetic investigation indicates that this complex is a SMM, which may extend the chemistry of MCs and polynuclear manganese clusters on both structures and the magnetic properties to some extent.

■ ASSOCIATED CONTENT

S Supporting Information. X-ray crystallographic data in CIF format, experimental procedures, additional structural plots,

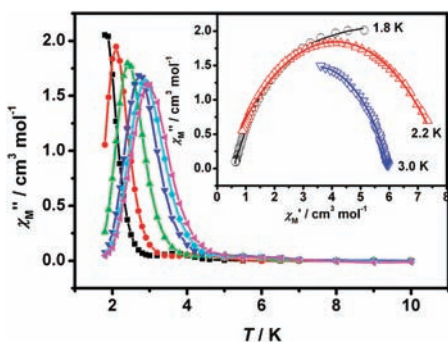


Figure 3. Plot of the in-phase (χ_M') and out-of-phase (χ_M'') ac susceptibility signals for **1**, recorded with frequencies of 1 (■), 10 (●), 100 (▲), 499 (▼), 997 (■), and 1488 (tilted ▲) Hz. Inset: Cole–Cole diagram for **1**. The solid line represents the least-squares fit by the Debye model.

plots of χ_M^{-1} vs T , plots of χ_M and χ_M'/T vs T , plot of $\ln(2\pi f)$ vs T_B^{-1} , and a table of BVS calculations. This material is available free of charge via the Internet at <http://pubs.acs.org>. Crystallographic data for the compound have also been deposited with the Cambridge Crystallographic Data Centre under CCDC 787699. The coordinates can be obtained, upon request, from the Director, Cambridge Crystallographic Data Centre, 12 Union Road, Cambridge CB2 1EZ, U.K.

AUTHOR INFORMATION

Corresponding Author

*E-mail: jmdou@lcu.edu.cn (J.D.), yousong@nju.edu.cn (Y.S.), lidacheng@lcu.edu.cn (D.L.).

ACKNOWLEDGMENT

We are thankful for financial support from the National Natural Science Foundation of China (Grants 20671048, 91022031, and 21041002), the Major State Basic Research Development Program (Grant 2007CB925102), and the Shandong “Taishan Scholar Research Fund”. XAFS data were collected at the Shanghai Synchrotron Radiation Facility, which is supported by the National Development and Reform Commission of China, Chinese Academy of Sciences, and Shanghai Municipal Government.

REFERENCES

- (a) Pecoraro, V. L. *Inorg. Chim. Acta* **1989**, *155*, 171. (b) Lah, M. S.; Pecoraro, V. L. *J. Am. Chem. Soc.* **1989**, *111*, 7258.
- (a) Bodwin, J. J.; Cutland-Van Noord, A. D.; Malkani, R. G.; Pecoraro, V. L. *Coord. Chem. Rev.* **2001**, *216–217*, 489. (b) Mezei, G.; Zaleski, C. M.; Pecoraro, V. L. *Chem. Rev.* **2007**, *107*, 4933 and references cited therein. (c) Prakash, M. J.; Lah, M. S. *Chem. Commun.* **2009**, 3326. (d) Psomas, G.; Dendrinou-Samara, C.; Alexiou, M.; Tsohos, A.; Raptopoulou, C. P.; Terzis, A.; Kessissoglou, D. P. *Inorg. Chem.* **1998**, *37*, 6556. (e) Psomas, G.; Stemmler, A. J.; Dendrinou-Samara, C.; Bodwin, J. J.; Schneider, M.; Alexiou, M.; Kampf, J. W.; Kessissoglou, D. P.; Pecoraro, V. L. *Inorg. Chem.* **2001**, *40*, 1562. (f) Dendrinou-Samara, C.; Psomas, G.; Iordanidis, L.; Tangoulis, V.; Kessissoglou, D. P. *Chem.—Eur. J.* **2001**, *5041*. (g) Tsvikias, I.; Alexiou, M.; Pantazaki, A. A.; Dendrinou-Samara, C.; Kyriakidis, D. A.; Kessissoglou, D. P. *Bioinorg. Chem.* **2003**, 85.
- (a) Liu, S. X.; Lin, S.; Lin, B. L.; Lin, C. C.; Huang, J. Q. *Angew. Chem., Int. Ed.* **2001**, *40*, 1084. (b) Moon, D.; Song, J.; Kim, B. J. B.; Suh, J.; Lah, M. S. *Inorg. Chem.* **2004**, *43*, 8230. (c) Dou, J. M.; Liu, M. L.; Li, D. C.; Wang, D. Q. *Eur. J. Inorg. Chem.* **2006**, 4866. (d) Lim, C. S.;

Cutland-Van Noord, A. D.; Kampf, J. W.; Pecoraro, V. L. *Eur. J. Inorg. Chem.* **2007**, 1347. (e) Choi, J.; Park, J.; Park, M.; Moon, D.; Lah, M. S. *Eur. J. Inorg. Chem.* **2008**, 5465.

(4) (a) Sessoli, R.; Gatteschi, D.; Caneschi, A.; Novak, M. A. *Nature* **1993**, *365*, 141. (b) Christou, G.; Gatteschi, D.; Hendrickson, D. N.; Sessoli, R. *MRS Bull.* **2000**, *25*, 66. (c) Gatteschi, D.; Sessoli, R. *Angew. Chem., Int. Ed.* **2003**, *42*, 268. (d) Aromil, G.; Brechin, E. K. *Struct. Bonding (Berlin)* **2006**, *122*, 1.

(5) (a) Ruiz, D.; Sun, Z.; Albelá, B.; Folting, K.; Ribas, J.; Christou, G.; Hendrickson, D. N. *Angew. Chem., Int. Ed.* **1998**, *37*, 300. (b) Oshio, H.; Nakano, M. *Chem.—Eur. J.* **2005**, *11*, 5178. (c) Ako, A. M.; Hewitt, I. J.; Mereacre, V.; Clérac, R.; Wernsdorfer, W.; Anson, C. E.; Powell, A. K. *Angew. Chem., Int. Ed.* **2006**, *45*, 4926. (d) Freedman, D. E.; Jenkins, D. M.; Iavarone, A. T.; Long, J. F. *J. Am. Chem. Soc.* **2008**, *130*, 2884. (e) Kostakis, G. E.; Ako, A. M.; Powell, A. K. *Chem. Soc. Rev.* **2010**, 2238.

(6) (a) Milios, C. J.; Whittaker, A. G.; Brechin, E. K. *Polyhedron* **2007**, *26*, 1927. (b) Milios, C. J.; Piligkos, S.; Brechin, E. K. *Dalton Trans.* **2008**, 1809. (c) Zaleski, C. M.; Depperman, E. C.; Kampf, J. W.; Kirk, M. L.; Pecoraro, V. L. *Inorg. Chem.* **2006**, *45*, 10022. (d) Zaleski, C. M.; Kampf, J. W.; Mallah, T.; Kirk, M. L.; Pecoraro, V. L. *Inorg. Chem.* **2007**, *46*, 1954.

(7) (a) Milios, C. J.; Raptopoulou, C. P.; Terzis, A.; Lloret, F.; Vicente, R.; Perlepes, S. P.; Escuer, A. *Angew. Chem., Int. Ed.* **2004**, *43*, 210. (b) Milios, C. J.; Vinslava, A.; Wood, A. P.; Parsons, S.; Wernsdorfer, W.; Christou, G.; Perlepes, S. P.; Brechin, E. K. *J. Am. Chem. Soc.* **2007**, *129*, 8. (c) Prescimone, A.; Milios, C. J.; Moggach, S.; Warren, J. E.; Lennie, A. R.; Sanchez-Benitez, J.; Kamenev, K.; Bircher, R.; Murrie, M.; Parsons, S.; Brechin, E. K. *Angew. Chem., Int. Ed.* **2008**, *47*, 2828. (d) Feng, P. L.; Stephenson, C. J.; Amjad, A.; Ogawa, G.; Barco, E.; Hendrickson, D. H. *Inorg. Chem.* **2010**, *49*, 1304.

(8) (a) Cutland-Van Noord, A. D.; Halfen, J. A.; Kampf, J. W.; Pecoraro, V. L. *J. Am. Chem. Soc.* **2001**, *123*, 6211. (b) Mezei, G.; Kampf, J. W.; Pan, S.; Poeppelmeier, K. R.; Watkins, B.; Pecoraro, V. L. *Chem. Commun.* **2007**, 1148. (c) Boron, T. T., III; Kampf, J. W.; Pecoraro, V. L. *Inorg. Chem.* **2010**, *49*, 9104.

(9) Crystal data for **1**: $C_{133}H_{173}Mn_{18}N_{17}O_{61}$, $M = 3974.80$, cubic, space group $I23$, $a = 26.050(2)$ Å, $V = 17677(3)$ Å³, $T = 173$ K, $Z = 8$, $D_c = 1.356$ g/cm³, $F(000) = 7312$, cryst dimens $0.13 \times 0.11 \times 0.11$ mm, $R1 = 0.0441$ and $wR2 = 0.1043$ for 2279 reflections with $I > 2\sigma(I)$, $GOF = 1.097$, largest peak/hole $0.66/-0.30$.

(10) (a) Bagai, R.; Abboud, K. A.; Christou, G. *Inorg. Chem.* **2008**, *47*, 621. (b) Manoli, M.; Collins, A.; Parsons, S.; Candini, A.; Evangelisti, M.; Brechin, E. K. *J. Am. Chem. Soc.* **2008**, *130*, 11129. (c) Jones, L. F.; Rajaraman, G.; Brockman, J.; Murugesu, M.; Sanudo, E. C.; Raftery, J.; Teat, S. J.; Wernsdorfer, W.; Christou, G.; Brechin, E. K.; Collison, D. *Chem.—Eur. J.* **2004**, *10*, 5180. (d) Jones, L. F.; Raftery, J.; Teat, S. J.; Collison, D.; Brechin, E. K. *Polyhedron* **2005**, *24*, 2443.

(11) (a) Brechin, E. K.; Soler, M.; Davidson, J.; Hendrickson, D. N.; Parsons, S.; Christou, G. *Chem. Commun.* **2002**, 2252. (b) Piligkos, S.; Rajaraman, G.; Soler, M.; Kirchner, N.; Slagere, J. V.; Bircher, R.; Parsons, S.; Gudel, H.-U.; Kortus, J.; Wernsdorfer, W.; Christou, G.; Brechin, E. K. *J. Am. Chem. Soc.* **2005**, *127*, 5572. (c) Mondal, K. C.; Song, Y.; Mukherjee, P. S. *Inorg. Chem.* **2007**, *46*, 9736. (d) Murugesu, M.; Wernsdorfer, W.; Christou, G.; Brechin, E. K. *Polyhedron* **2007**, *26*, 1845. (e) Koumoussi, E. S.; Manos, M. J.; Lampropoulos, C.; Tasiopoulos, A. J.; Wernsdorfer, W.; Christou, G.; Stamatatos, T. C. *Inorg. Chem.* **2010**, *49*, 3077.

(12) Feng, Y. H.; Wang, C.; Zhao, Y. F.; Liao, D. Z.; Yan, S. P.; Wang, Q. L. *Inorg. Chim. Acta* **2009**, *362*, 3563 and references cited therein.

(13) (a) Mydosh, J. A. *Spin Glasses: An Experimental Introduction*; Taylor and Francis: London, 1993. (b) Wang, S.; Zuo, J. L.; Gao, S.; Song, Y.; Zhou, H. C.; Zhang, Y. Z.; You, X. Z. *J. Am. Chem. Soc.* **2004**, *126*, 8900. (c) Ishii, N.; Okamura, Y.; Chiba, S.; Nogami, T.; Ishida, T. *J. Am. Chem. Soc.* **2008**, *130*, 24.